

Locational Marginal Emissions for Carbon-Aware Data Center Operations in Large-Scale Power Grids

1
2
3
Luc Cote¹ and Andy Sun^{1, 2*}

4
5
6
¹Operations Research Center, Massachusetts Institute of Technology, Cambridge, MA, USA

²Sloan School of Management, Massachusetts Institute of Technology, Cambridge, MA, USA

^{*}Correspondence: sunx@mit.edu

SUMMARY

7
8
9
10
11
12
13
14
15
16
17
18
19
20
Carbon accounting methods for electricity consumption face challenges regarding physical de-
liverability, double counting, additionality, and impact magnitude. Locational Marginal Emissions
(LMEs) show potential to address many of these key issues. However, their use in a large-scale
power grids remains understudied. We analyze the properties of LMEs from a data center's per-
spective in a 1493-bus Western Interconnection over one year of hourly operation. We find that
LME characteristics create three distinct regions: the hydropower-dominated Pacific Northwest,
with low and stable LMEs; the coal-heavy Intermountain West, containing often high LMEs; and the
Sunbelt, where mixed generation leads to variable LMEs correlated with solar output. This
characterization provides analytical guidance for data center emission reduction. In particular,
LME-guided emission reduction interventions through data center temporal-spatial load shifting,
siting, and renewable procurement display over 85% accuracy with respect to actual emission
reduction. Moreover, large-scale, nodal grid simulation is shown to be critical to accurate evalua-
tion.

KEYWORDS

21
Locational marginal emission, carbon accounting, large-scale power systems, data centers

INTRODUCTION

22
23
24
25
26
27
28
29
As the modern AI economy unfolds, worldwide energy grids are experiencing a surge in data
center energy demand just as many nations have begun to reconfigure their energy grids for
the renewable transition. Without proper alignment of this massive new data center demand
and green grid development, countries risk missing key emissions targets and undoing global
climate progress. Indeed, in recent years, countries experiencing data center growth have seen
an increase in the energy demand of these facilities outpace the addition of renewable capacity
to their grids, contributing to recent failures to reach EU climate targets^{1,2}.

30
31
32
33
In spite of such misalignment, many of the same companies driving this increase in demand
have also shown a commitment to reduced-emission goals in the form of net-zero targets. To
achieve these net-zero goals, data center operators can rely on three major forms of intervention:

1. **data center siting** - the intentional placement of data centers in areas where low-carbon
34
energy resources are readily available to meet demand,
2. **renewable procurement** - the funding of grid upgrade and low carbon generation projects
35
to displace carbon emissions, and

3. **data center operations** - the geographic and temporal shift of data center workloads toward areas and periods of low carbon production.

Data center siting and renewable procurement are both types of facility siting decisions and have seen implementation through different forms of scope 2¹ carbon accounting practices, with data center companies adopting multiple types of carbon accounting policies. In fact, many of the largest data center stakeholders, including Amazon³, Google⁴, Meta⁵, and Microsoft⁶ publicize their renewable energy procurement and data center location strategies. Furthermore, recent demand-shifting strategies involving data center-driven work loads have shown an ability to participate significantly in demand response programs both in academic studies⁷ and in practice⁸.

However, although such scope 2 interventions enable companies to achieve net zero carbon goals, it is not clear that such interventions reliably work to decrease carbon emissions. Current scope 2 emissions accounting practices have seen significant criticism in recent years, stemming from challenges regarding deliverability, double counting, additionality, and impact magnitude⁹⁻¹³. Furthermore, recent work has shown data center demand response can lead to negligible emission changes or even increases in system emissions^{14,15}.

Locational Marginal Emissions One tool that has been identified to provide possible improvements in intervention choice is the use of locational marginal emissions (hereafter, LMEs) which describe the impact of changes in load on the system-wide carbon emissions within an electric power grid¹⁶. More formally, we define the LME corresponding to node n in a power grid as

Definition 1

$$LME_n := \frac{d \text{ System Emissions}}{d \text{ Load}_n}, \quad (1)$$

where System Emissions refers to the CO₂ output of the entire energy grid and Load _{n} refers to the net power load at node n , which is the difference of load and generation at that node. The physical unit of LME _{n} is MMT CO₂/MWh or kgCO₂/MWh². LMEs have also been used to define carbon accounting systems that tie together emission attribution and intervention evaluation^{17,18} with the following carbon accounting scheme:

Definition 2 Carbon accounts,

- **load:** $LME_n \times load_n$ - the carbon account for a load is defined as the nodal marginal emissions rate multiplied by the load's total magnitude,
- **generator:** $(carbon\ intensity_g - LME_g) \times generation_g$ - the carbon account for a generation unit is defined as the difference between the generator's unit emission rate and the nodal marginal emissions rate multiplied by the total generation,
- **transmission:** $SCI_\ell \times line\ flow_\ell$ - here, SCI_ℓ refers to the "shadow carbon intensity" of a transmission line which describes how the system emissions would change with respect to a change in the line's power limit and line flow _{ℓ} refers to the magnitude of the power delivered through line ℓ .

LME-based accounting methods have been shown to have many desirable properties regarding the issues present in current scope 2 accounting practices. Of particular note is the aptly

¹scope 2 emissions refer to the attribution of indirect emissions to the consumption of electricity, heating, and cooling.

²MMT stands for million metric tons, kg stands for kilograms, and MWh stands for megawatt hours.

named “Carbon Accounting Theorem”^{17,18} which states that the total emissions accounts across all load, generation, and transmission entities as described in Definition 2 sum to the total scope 1 emissions of the energy grid, allowing such accounting schemes to address double counting issues.

Definition 3 *Carbon accounting theorem,*

$$\sum_n LME_n \times load_n + \sum_g (carbon\ intensity_g - LME_g) \times generation_g + \sum_{\ell} SCI_{\ell} \times line\ flow_{\ell} = system\ emissions. \quad (2)$$

Furthermore, LMEs are nodal properties whose definition is based on the response of the grid, and subsequently, the grid congestion that constrains this response is closely related to this calculation^{17,18}, enabling LME-based accounting to resolve deliverability issues.

Contributions In this paper, we seek to evaluate the LME characteristics of a large interconnection in the United States and answer how a data center operator might use LMEs and LME-based accounting to guide emission reduction interventions. In particular, we make the following two main contributions:

1. investigate broad carbon intervention insights given by the empirical properties of LMEs and LME-based accounting using a high-granularity representation of the WECC grid,
2. evaluate the accuracy and utility of LMEs as indicators within the WECC grid for the resulting emission changes from interventions of data center siting, renewable procurement, and data center operations.

Empirical Properties: We apply a novel optimization-based LME calculation methodology to a 1493-bus realistic representation of the WECC grid with hourly dispatches simulated over 1 year of generation and load data, providing a fine-grained, interconnection-scale survey of grid LMEs. Through such experiments, we analyze the regional, hourly, and seasonal patterns of WECC LMEs and how these patterns are reflected across LME-based carbon accounts. Furthermore, we consider how such results provide insights for a carbon-conscious energy consumer’s operations.

Accuracy Evaluation: We extend our simulation experiments to consider the three main LME-based intervention strategies for data centers of consumption siting, renewable procurement, and data center operations. For operations and consumption siting, we consider the lens of a data center operator with large data centers of 100 and 200 MW spanning the WECC grid, while for renewable procurement, we take the perspective of a renewable energy developer performing generation siting of a 100MW zero-carbon resource. In all three cases, we find that LMEs serve as an accurate metric for describing intervention results.

RESULTS

In the following experiments, we use a realistic representation of the modern WECC grid to investigate the empirical properties of the described LME calculation and accounting methodology. To create such a representation of the WECC grid, we follow the methodology outlined in Lee and Sun¹⁹, using Open Street Map data²⁰ along with 2023 EIA 860²¹ generation and substation location data to estimate the transmission properties of the WECC 230 KV grid. This leads to a grid with the characteristics described in Table 1. Additionally, we use historic load and weather

Entity	Bus	Line	Load	Coal	Gas	Wind	Solar	Nuclear	Hydro
Number of elements	1493	1919	722	25	180	90	58	3	70
Installed Capacity (GW)	N/A	4357.1	122.5	22.5	86.6	25.9	21.5	7.7	37.9
Emissions (kgCO ₂ /MWh)	N/A	N/A	N/A	800	450	0	0	0	0

Table 1: Makeup of the simulated WECC grid

data, once again defined in the manner of Lee and Sun¹⁹, to define a representative year of WECC hourly dispatch periods, each period defined by scaling factors for nodal loads and variable renewable energy (VRE) capacity factors. The weather data describes the hourly conditions of 2016 at 20km resolution and is sourced from NOAA²², while the load data is sourced from the 2023 EIA 930 dataset²³, which describes the hourly profiles across the WECC area.

To observe and quantify regional trends, we additionally refer to the EPA IPM regions across the WECC. In Figure 1, we visualize how each region corresponds to the buses within the simulated WECC grid.

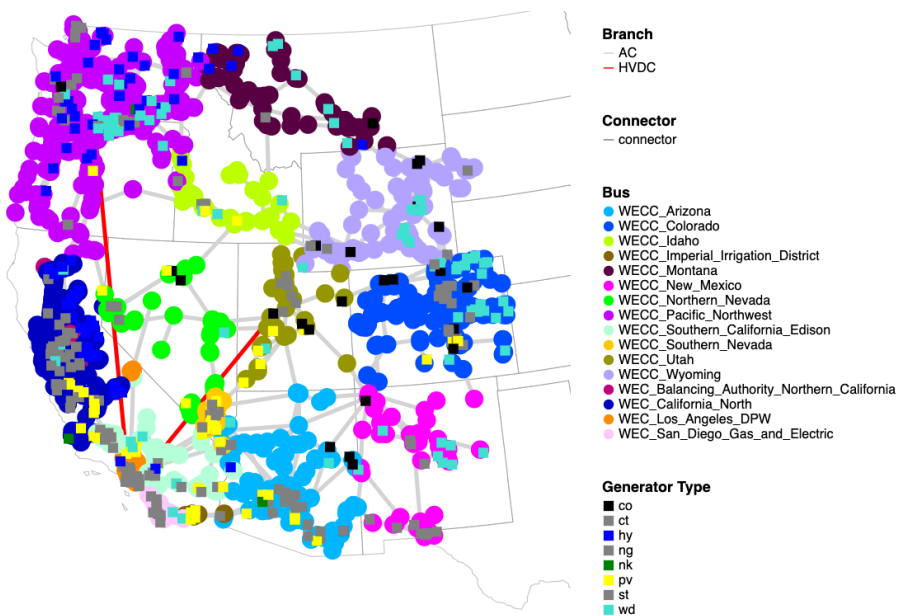


Figure 1: EPA IPM Planning Regions over the WECC Data

LMEs Reveal Three Regional Characteristics within WECC

The WECC grid spans a wide geographic area with a diverse set of climates and policies, leading to significant differences in energy demands and generation resources across regions. Broadly speaking, our grid simulation reveals that WECC regions can be grouped into three main types of LME characteristics whose correlation strength we evaluate in Figure 3.

Pacific Northwest and Montana IPM Regions make up the blue sections in the north of Figure 2, experiencing consistently low LMEs with an overall area average LME of ≈ 90 kgCO₂/MWh. This low LME pattern comes from a high proportion of time with zero carbon generation acting as the marginal generation resource due to a stable supply of hydropower along with significant amounts of wind capacity. An exception to this trend occurs in the southern portion of region, where a less abundant hydro supply combined with some transmission congestion from the north causes nearby natural gas plants to act as the marginal resource at times.

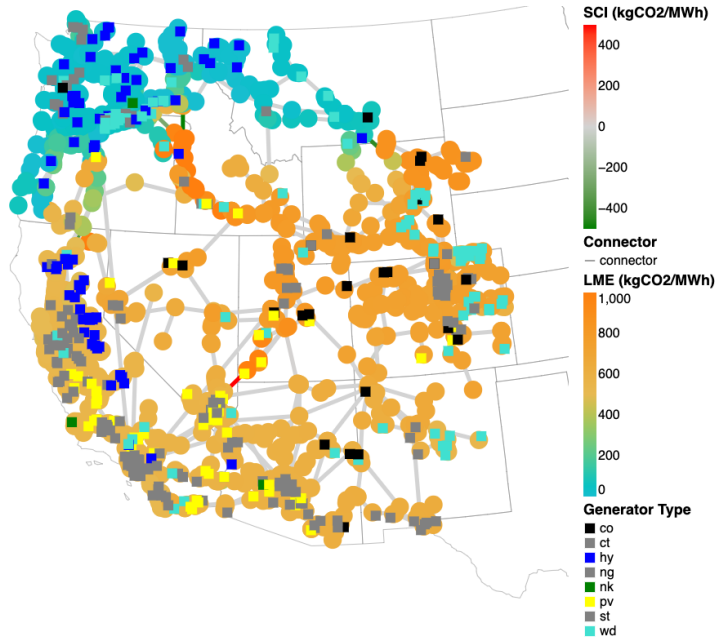


Figure 2: Average locational marginal emissions and shadow carbon intensities over the experimental horizon.

The “Inter-Mountain West” IPM regions of Idaho, Wyoming, Colorado, and Utah make up the clusters of darker orange nodes in the center and east of Figure 2, exhibiting high average LMEs with an area overall average of ≈ 710 kgCO₂/MWh. These regions contain some renewable development in the forms of wind and solar; however, they lack sufficient capacity to completely satisfy the regional load during most hours, leading to a tendency for fossil fuel generation to act as the marginal resource. Furthermore, these regions contain significant coal plant capacity, which exhibits emission rates much higher than those of natural gas plants, resulting in high regional LMEs. This region experiences some levels of transmission congestion within the Cheyenne-Denver corridor, where transmission lines between nearby wind farms and the urban areas exhibit negative SCIs³, implying congestion limiting wind dispatch. Similarly, the lines connecting the hydropower and wind resources of the PNW and Montana to this region tend to exhibit negative LMEs, reflected in the dark green lines connecting western Washington to Idaho and Western Montana to Wyoming in Figure 2.

Finally, the remaining “Sunbelt” IPM regions make up the lighter orange nodes in the south and west of Figure 2, exhibiting variable LMEs which follow trends related to solar radiation strength. Such trends can reasonably be explained from high levels of solar production within the regions. Some areas within these regions, such as northern and southern California, contained limited access to coal plants and higher levels of solar development, leading to lower average LMEs along with more pronounced solar trends, compared to other areas such as New Mexico which contain higher coal access along with a more limited solar supply. These regions exhibited mixed congestion with some lines connecting renewables to high demand areas such as from the low-carbon PNW to northern California experiencing negative SCIs, but also lines connecting to coal generation in Utah and New Mexico exhibiting positive SCIs (see the red line northeast of southern Nevada in Figure 2), indicating the existence of some coal-limiting congestion leading to an increase in natural gas dispatch.

This three-region grouping of IPM regions is further reflected through observing the correlation

³SCIs refers to the change in system carbon emissions resulting from a change in transmission line capacity as described in Definition 2.

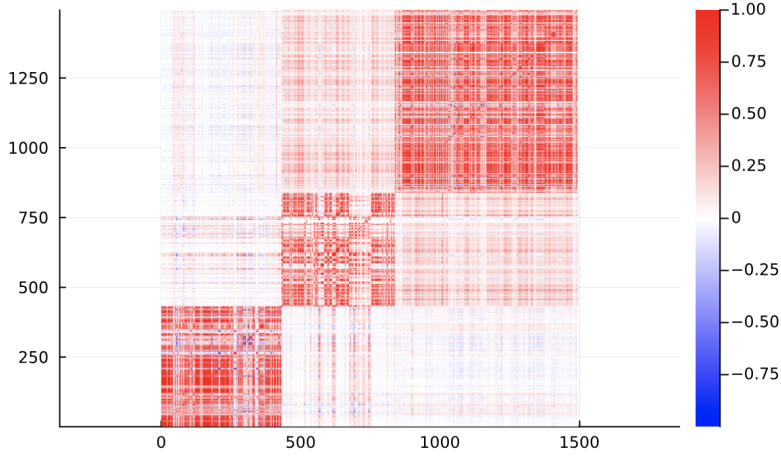


Figure 3: Heatmap of the Pearson correlation coefficients between nodal LMEs. Nodes 1-431 belong to the “Mountain West” regions, nodes 432-837 belong to the Pacific Northwest and Montana regions, and nodes 838-1493 belong to “Sunbelt” regions.

tions between nodal vectors of LMEs over time. Figure 3 displays a clear three block diagonal structure outlining high intra-regional correlation. Furthermore, we can use such correlation data to create a distance function between buses in the form of

$$d_{ij} = 1 - |\text{correlation}(i, j)|, \quad (3)$$

to give a measure of the temporal pattern distance between nodes. Combining this distance metric with the rescaled difference magnitude between bus average LMEs allows for the creation of a distance function which reflects the LME characteristics over time

$$\tilde{d}_{ij} = \frac{1}{2} d_{ij} + \frac{1}{2} \frac{|\bar{\text{LME}}_i - \bar{\text{LME}}_j|}{\max_{i',j'} |\bar{\text{LME}}_{i'} - \bar{\text{LME}}_{j'}|}, \quad (4)$$

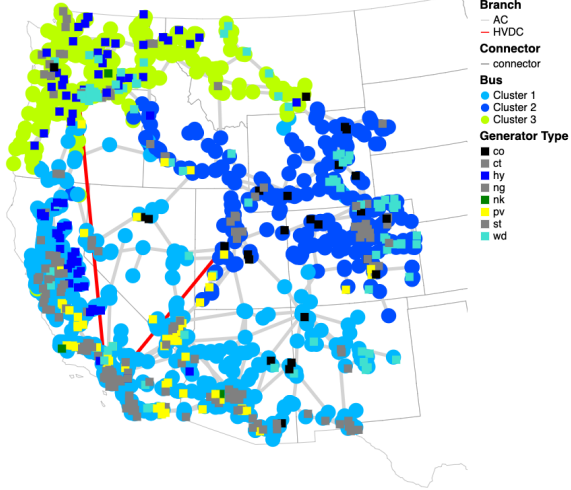
which can be used to perform hierarchical clustering among buses²⁴. Indeed, in Figure 4a such a hierarchical clustering recovers a bus grouping quite similar to the three region IPM grouping, while in Figure 4b the dendrogram created from such a clustering confirms $k = 2$ and $k = 3$ groups to be natural clustering choices.

LMEs Reflect Hourly and Seasonal Generation Characteristics

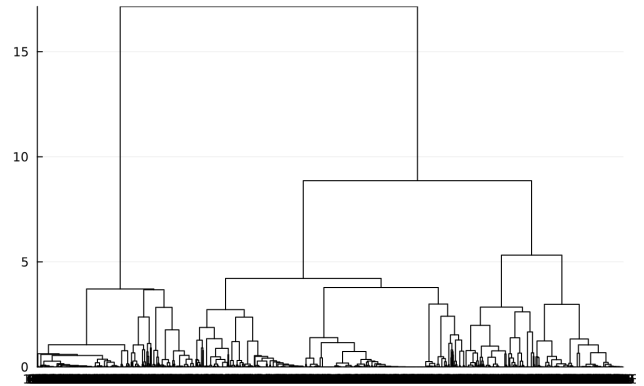
The hourly and seasonal trends of LMEs within the WECC grid remain well grouped into the three broad LME characteristic types.

Due to the significantly higher temporal correlation of solar production when compared to wind, the hourly trends of LMEs across the WECC seem to be driven by the interplay of solar production and net load. In general, despite an overall increasing load through the afternoon as shown in Figure 5a, the “Inter-Mountain West” and “Sunbelt” regions experience slight dips in average LMEs in Figure 6a, likely due to the significant increase in solar production occurring at this time outpacing the demand increases. This increased solar production also leads to a decrease in net load in these regions, decreasing some of the congestion occurring in lines from the PNW region into northern California and into Idaho along with lines from Utah to southern Nevada as seen in Figure 7.

The monthly LME trends are similarly dominated by solar production trends (see Figure 5b- Figure 6b), with higher solar production levels of the summer months leading to significantly

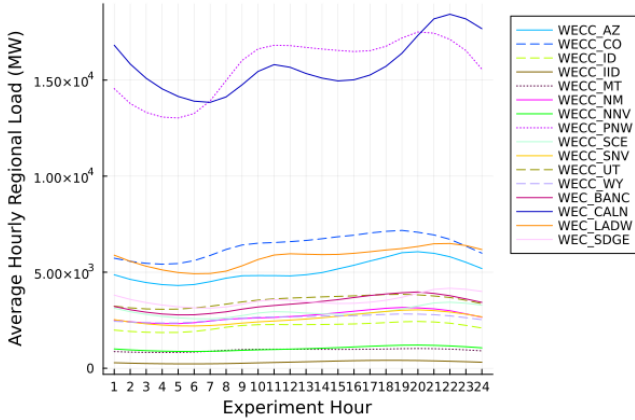


(a) Bus groups recovered for $k = 3$ groups.

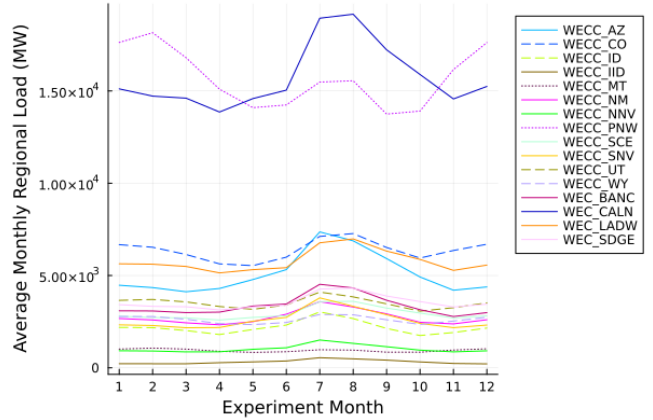


(b) Clustering dendrogram describing total internal variance across all clusters.

Figure 4: Results from hierarchical clustering of bus groups using distance (4) and ward's method for linkage



(a) hourly demand

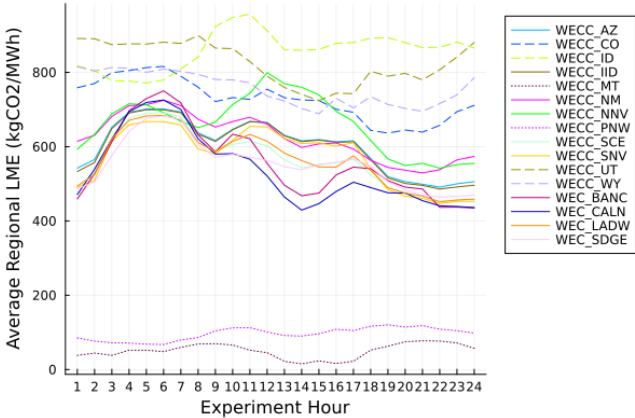


(b) monthly demand

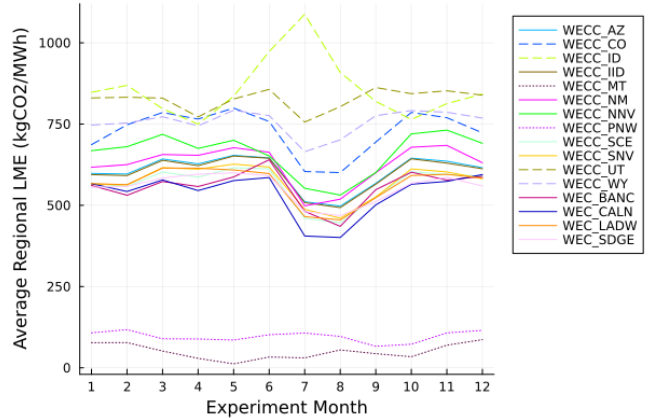
Figure 5: Average power demand of the WECC EPA IPM regions over hourly and monthly periods.

decreased LMEs across the “Inter-Mountain West” and “Sunbelt” regions, despite a net increase in demand (likely driven by cooling systems) during these months. Interestingly, some southern portions of the PNW region also experience a slight decrease in LMEs during these months (see Figure 8), likely driven by a combination of decreasing demand in the PNW region during the summer months and a decreased demand for energy exports from increased solar production in California. It is also worth noting that the Idaho region remains an exception to the trend of decreasing LMEs in the summer months, showing a regional average LME actually higher than that of coal plants, indicating that consumption in the region is likely causing increased fossil fuel dispatch and decreased renewable dispatch through a combination of regional congestion and the physics of power flows.

183
184
185
186
187
188
189
190
191
192



(a) hourly LMEs



(b) monthly LMEs

Figure 6: Average locational marginal emissions of the WECC EPA IPM regions over hourly and monthly periods.

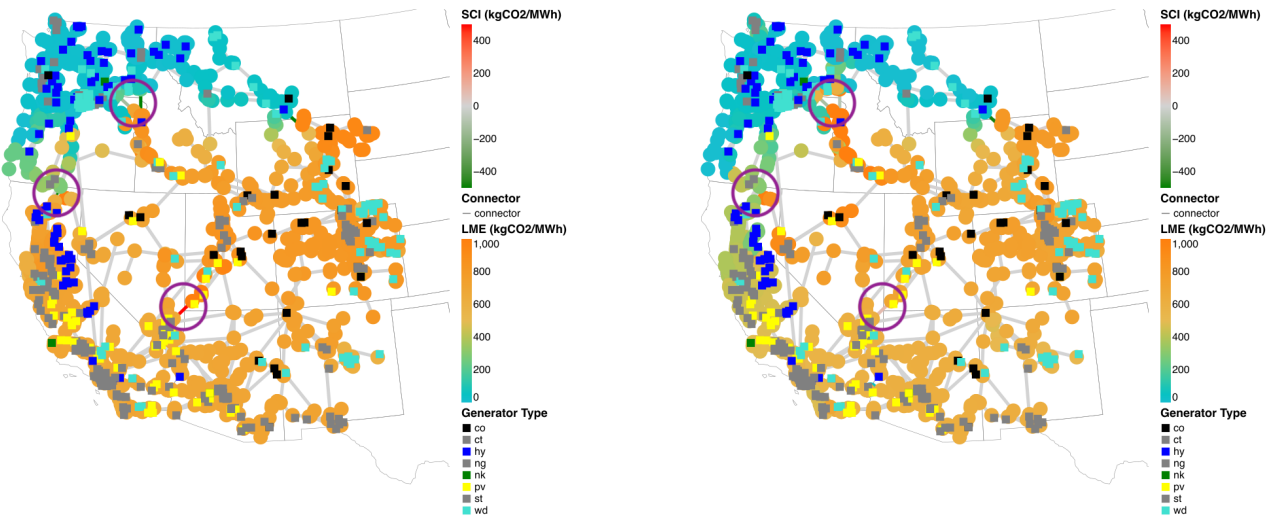


Figure 7: Average locational marginal emissions and shadow carbon intensities over the experimental year at 5am (left) and 2pm (right). Areas with transmission lines which experience significant hourly differences are circled in purple for clarity.

LMEs Balance System Emissions and Reflect Entity Level Impacts

193

In this section, we apply the LME-based accounting scheme in the manner of LME-Based Carbon Accounting Calculation. This scheme provides individual carbon accounts for all grid entities including loads, generation, and transmission.

194

Over the course of the experiment, we observed a total of 125.9 million metric tons (MMT) of scope 1 carbon emissions from generation resources. Applying an LME-based accounting framework, we observe that this translates into a carbon account of 419.1 MMT ascribed to the grid load, a net total of -146.6 MMT ascribed to generation resources, and a total of -146.6 MMT ascribed to transmission infrastructure. This yields a total of 125.9 MMT of carbon emissions across all carbon accounts, directly matching the scope 1 emissions of the grid dispatch.

195

The large magnitude of load-attributed LME-based emissions accounts is notable, with the total load carbon account summing to almost 3 times the scope 1 carbon emissions of the WECC grid. This is indicative of a grid with high amounts of renewable production without saturation,

196

197

198

199

200

201

202

203

204

205

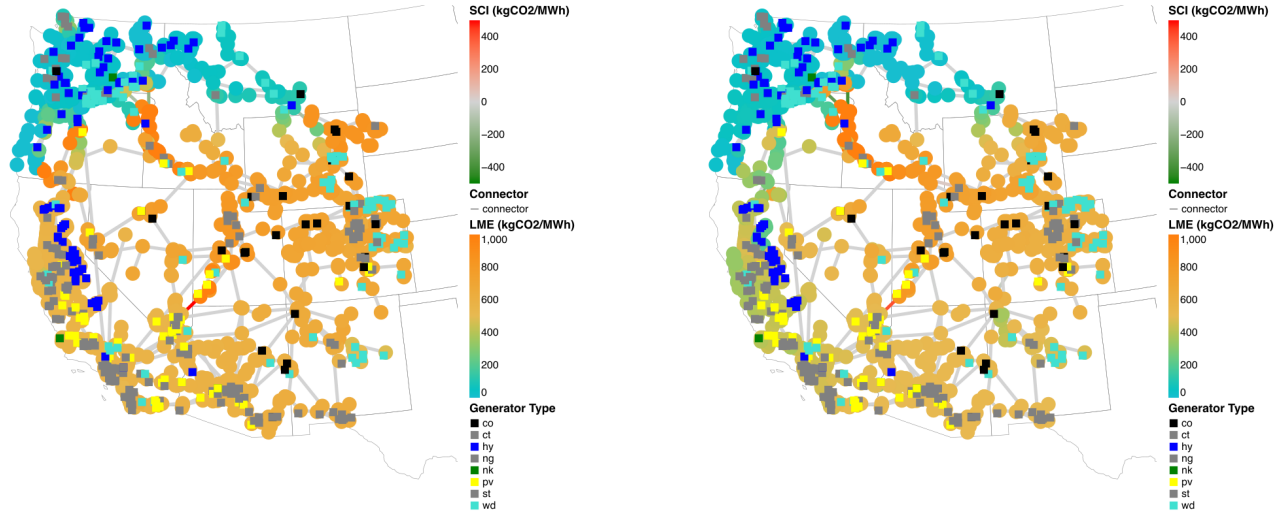


Figure 8: Average locational marginal emissions and shadow carbon intensities over the experimental month in January (left) and July (right).

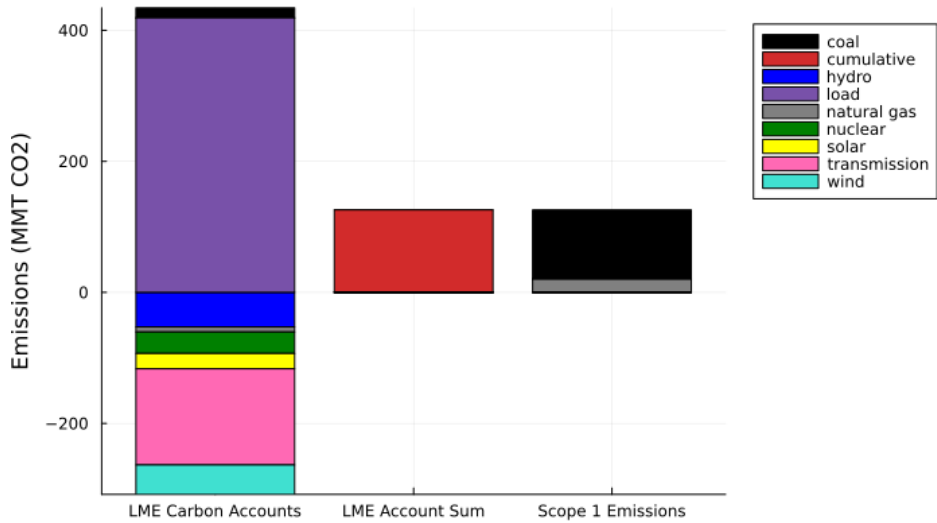


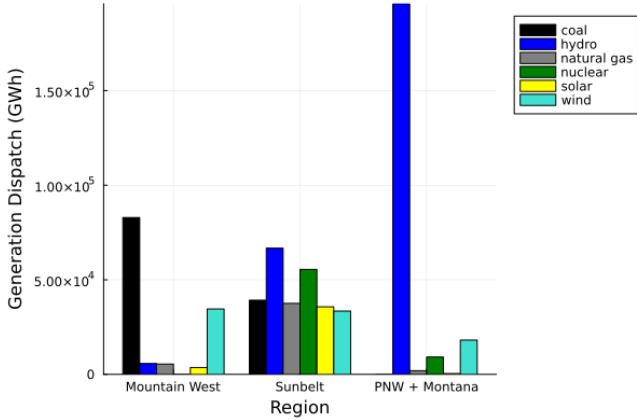
Figure 9: Total carbon accounts over the experimental horizon.

Generation Type	Coal	Gas	Nuclear	Wind	Solar	Hydro
Carbon Account (MMT CO ₂)	15.2	-7.7	-32.8	-45.0	-23.5	-52.7
Dispatch (GWh)	122,131	41,876	64,666	86,153	39,744	268,392
Scope 1 Emissions (MMT CO ₂)	105.6	20.2	-	-	-	-

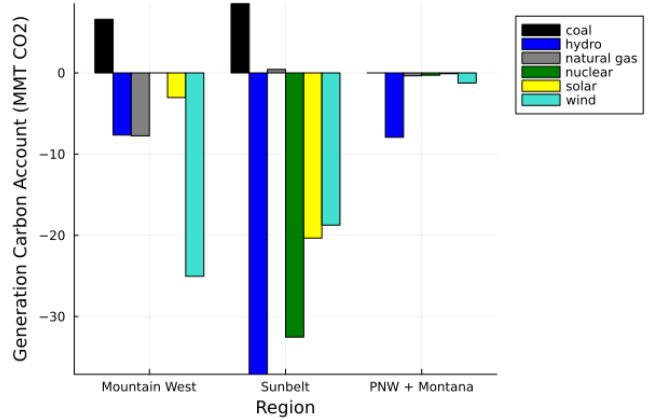
Table 2: Generation resource carbon accounts and total power production over the experimental horizon.

i.e., despite higher production levels, renewables do not spend much time acting as a marginal generation resource, causing the load to be assigned carbon emissions at a rate higher than the grid average emission factor⁴. In this instance, we observe the average LME-based emissions account intensity to be ≈ 672 kgCO₂/MWh, roughly halfway between the carbon intensities of nat-

⁴Grid average emission factor refers to the total emissions of the entire power grid system divided by the total power produced by the system.



(a) dispatch



(b) carbon accounts

Figure 10: Total generation dispatch and carbon accounts by LME characteristic groups over the experiment year.

ural gas and coal, indicating a general tendency of fossil fuel plants to be the marginal resources across the entirety of WECC, while the grid average emission factor is $\approx 202 \text{ kgCO}_2/\text{MWh}$, or roughly halfway in between the carbon intensities of renewables and natural gas, indicating a significant presence of renewables in the overall generation mix.

Dividing the net generation account into each fuel type, we see that coal generation experiences the only positive carbon account with a total of 15.2 MMT carbon emissions while natural gas production received a negative carbon account of -7.7 MMT CO_2 despite being a scope 1 emissions source (Table 2). However, in general, both coal and natural gas carbon accounts are quite small in magnitude compared to all other grid entities (Figure 9), indicating that such fossil resources spend most of their time on the margin.

Upon closer inspection of the generation accounting at the regional level we see that the negative carbon account of natural gas is driven by the coal-heavy “Mountain West” region, despite natural gas having a much larger dispatch footprint within the “Sunbelt” regions (Figure 10). Furthermore, we observe that the intensity of the mountain west natural gas carbon account is -1423 MT CO_2/GWh , much higher than the difference between natural gas and coal generation carbon intensity ($\approx 350 \text{ MT CO}_2/\text{GWh}$). When considering the dispatch cost ordering of generators within the simulation (coal being cheaper than gas), this indicates that the negative gas carbon accounts present in this region likely stems from natural gas plants being used to relieve regional congestion and thus enable an increased dispatch of renewables.

Additionally, while, in total, the transmission accounts experience a significant net negative, we observe a distribution of positive and negative carbon accounts across transmission infrastructure. Lines whose congestion limits the dispatch of coal and necessitates an increased dispatch of natural gas receive positive carbon accounts. This indicates that their upgrade would allow for more coal generation, and thus lead to an increase in emissions. Lines whose congestion limits the dispatch of renewable resources receive negative carbon accounts, indicating that their upgrade would result in a decrease in emissions. Here, we once again observe lines connecting the low carbon PNW and Montana regions to California (darker green lines in the center-west of Figure 11) and “Intermountain West” (lighter green lines connecting PNW to Idaho and Montana to Wyoming in Figure 11) to experience negative carbon accounts, implying the existence of significant congestion and the possibility of carbon (and cost) reducing upgrades. Furthermore, we observe that congestion is not entirely renewable limiting and we observe some lines to experience positive carbon accounts - particularly those connecting the coal-margin “Intermountain West” to the often gas-margin “Sunbelt” regions (see red lines connecting Utah to Nevada and

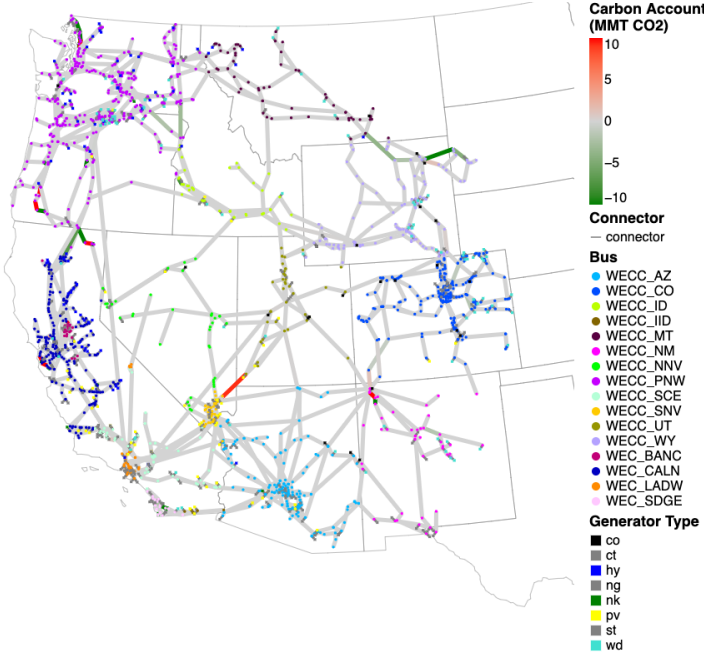


Figure 11: Total transmission carbon accounts over the experimental horizon.

Colorado to New Mexico in Figure 11). The existence of both positive and negative carbon accounts across the WECC transmission system suggests the importance of a principled upgrade strategy and the benefit that indicators such as the shadow carbon rent can provide for actors wishing to improve a transmission network to encourage decarbonization.

LMEs Provide Accurate Emission Signals for Data Center Operations

Carbon Signal Based Operation In the following experiments, we evaluate the use of LMEs for carbon-based demand response programs. In particular, we consider a data center operator with eight data centers located in regions with high expected data center future load, as projected by NREL²⁵. We perform four distinct experiments, varying the base load size of the data centers,

Location	San Francisco	Los Angeles	Sacramento	Reno	Salt Lake	Phoenix	Denver	Seattle
Bus #	1167	67	800	292	25	205	322	28
Load #	594	48	438	158	19	108	173	21

Table 3: Selected data center locations

the data center operating regions, and considering a grid-wide operator with control over all eight data centers vs. an operator localized to California, considering only the San Francisco, Los Angeles, and Sacramento data center locations. The explicit details of each experiment setup are summarized in Table 4.

For all experiments, we assume that up to 20% of a data center's load may be shifted as demand response. Shifted loads must be realized within the same day, and no data center load can exceed an additional 20% of baseload at any time⁵, i.e. for a 100MW baseload data center its load may be shifted to take on any value between 80MW and 120MW during any dispatch period.

⁵The 20% shifting assumption is seen in other academic work¹⁴ and based on the results of data center load shifting trials at Oracle which reported an ability to decrease load by 25%⁸.

Experiment	Exp 1	Exp 2	Exp 3	Exp 4
Data Center Regions	WECC	CA	WECC	CA
Data Centers	8	3	8	3
Data Center Size (MW)	100	100	200	200
Expected Change (MT CO ₂)	-4,168	-1,292	-7,731	-2,299
Realized Change (MT CO ₂)	-3,833	-1,151	-6,860	-1,971
Change Ratio	92%	89%	89%	86%

Table 4: data center shifting experiment descriptions and results

For each experiment the WECC dispatch is first reran with the addition of the experiment's data centers as static base loads, referred to as the "base case". The data center operator then solves a load shifting optimization problem, where they seek to minimize the sum of hourly LMEs at each data center node (given by the base case) multiplied by the data center loads at each hour. The difference between the hourly LMEs multiplied by the base load and the optimal objective of this problem is considered to be the expected shift in overall system emissions resulting from the application of such carbon-aware demand response

$$\text{expected change} := \sum_{t,dc} \text{load shift}_{t,dc} \times \text{LME}_{t,dc}, \quad (5)$$

while the total carbon emissions of the grid resulting from the economic dispatch of the shifted loads minus the realized carbon emissions from the economic dispatch of the base case describe the realized change in emissions

$$\text{realized change} := \text{shifted dispatch emissions} - \text{base case emissions}. \quad (6)$$

The results of each experiment are summarized in the bottom three rows in Table 4. In all experiments, LMEs provided an accurate estimate of the true system response with respect to data center load shifting, with the true response resulting in close to 90% ratio of the LME-derived expected emissions change.

Observing the differences between experiments, we see that the inclusion of geographically varied load shifting options has an outsized impact on the carbon-reduction ability of LME-based load-shedding schemes, with experiment 1 leading to a realized change of 333% of that of experiment 2, despite having only 267% more controllable load. This trend is repeated in experiments 3 and 4 with experiment 3 containing a realized shift of 348% that of experiment 4. Intuitively, such advantages come from the additional arbitrage opportunity which exists between regions with differing LME characteristics, especially if such regions have differing temporal patterns. Of additional note is that the increase in data center size seems to have a diminishing impact, with 179% and 171% difference in realized change between experiments 1 and 3 and experiments 2 and 4, respectively, despite a doubling of the shiftable data center load. Here, such differences can likely be explained by the increase in system-wide LMEs caused by the increased overall load from the increased data center size leading to fewer time periods where renewable capacity is sufficient in comparison to load to act as the marginal resource.

We can also consider the operational trends across the data centers within these experiments. As one might expect, the data center hourly load shifting patterns were highly correlated with the LME patterns for each region. The consistent low LMEs of the PNW led to a stable increased load for the Seattle data center over all experiment hours, while the rest of the data centers - located in the more variable "Sun Belt" and "Intermountain-West" regions shifted toward off-peak demand hours of the later night and early morning. Interestingly, we do not observe a significant shift towards off-peak midday hours as well, where high levels of solar production

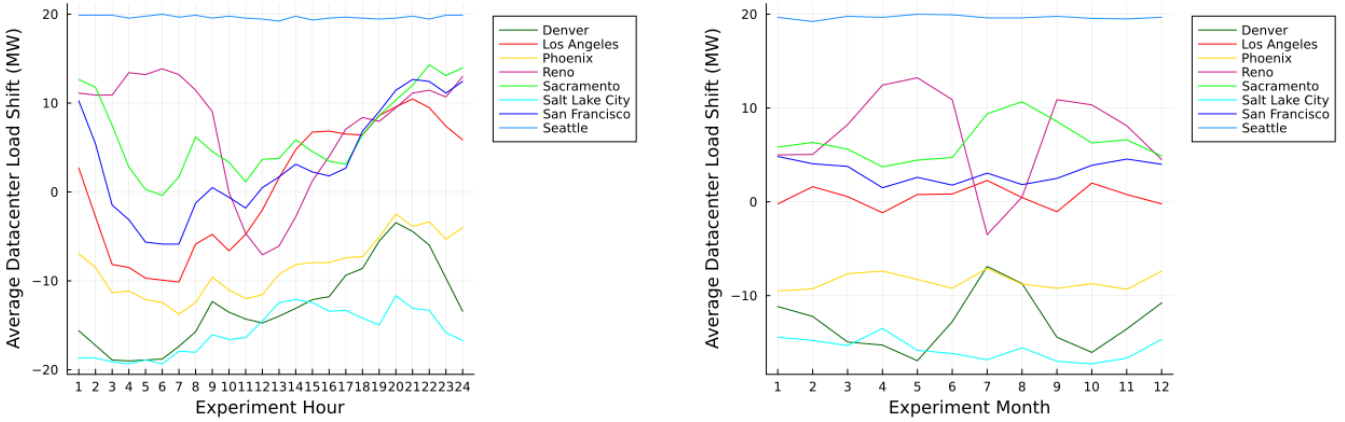


Figure 12: Average hourly (left) and monthly (right) load shift factors for each data center in experiment 1.

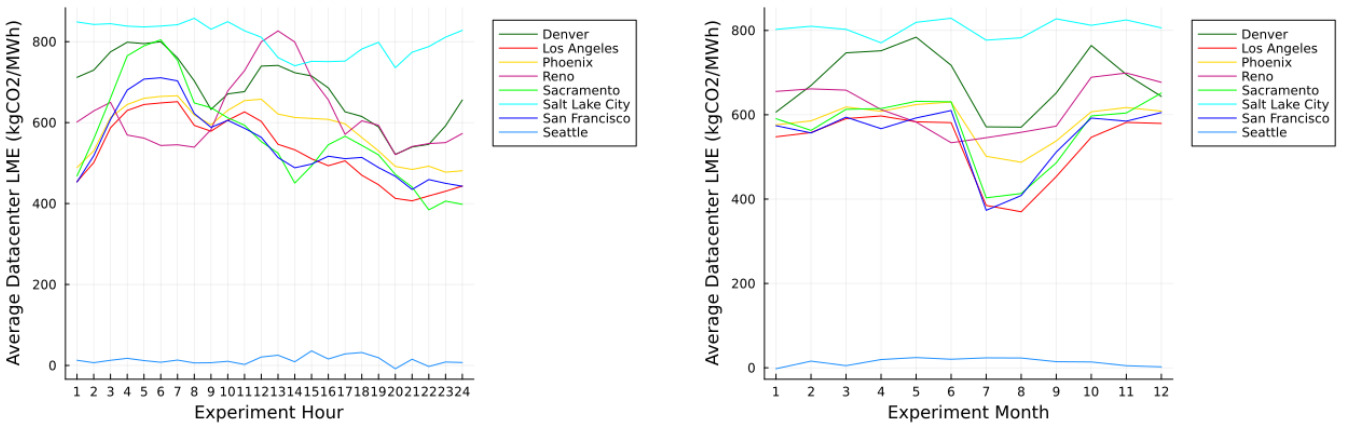


Figure 13: Average hourly (left) and monthly (right) LMEs for each data center bus in experiment 1.

were shown to lower the LMEs of such regions. This is likely due to the urban, high-demand area siting of these data centers, causing them to be downstream of any congestion curtailing renewable production and thus less likely to have decreased LMEs during times of higher renewable production. Indeed, when observing the LME trends of the data center buses (Figure 13) we observe that the pattern of midday LME drops from solar production does not exist for most buses with the exception of Sacramento.

However, unlike the hourly case, when considering the monthly LME patterns of the data center buses we see the observed regional seasonal patterns remain true. Due to the 24-hour constrained shifting window, such seasonal patterns are not directly reflected in terms of load distribution. Rather, as the summer increase in solar production and subsequent decrease in LMEs has a differing magnitude of impact on different data center buses, the LME-based ordering of data centers changes and is thus reflected in the seasonal load shifting patterns.

Economic Signal Based Operation Data center operation is not constrained to only follow emissions signals, and is incentivized in many markets to follow economic signals given by locational marginal prices (LMPs). Previous literature has explored such data center operation and found that such operation may lead to higher system-level emissions. Indeed, when rerunning experiment 1 using LMPs as a shifting signal rather than LMEs we found that while system cost decreased by $\approx 5\%$, system emissions increased by 78.5 MT CO₂. These emission increases

are likely driven by the economically incentivized shifting of power away from “Sunbelt” data centers and into “Mountain West” data centers due to the lower fuel price (yet higher emissions) of coal in comparison to natural gas which is often marginal in the “Sunbelt” regions. Such intuition is corroborated in Figure 14 where we see significant shifts away from Los Angeles and Reno data centers and significant positive shifts into Salt Lake City and Denver data centers.

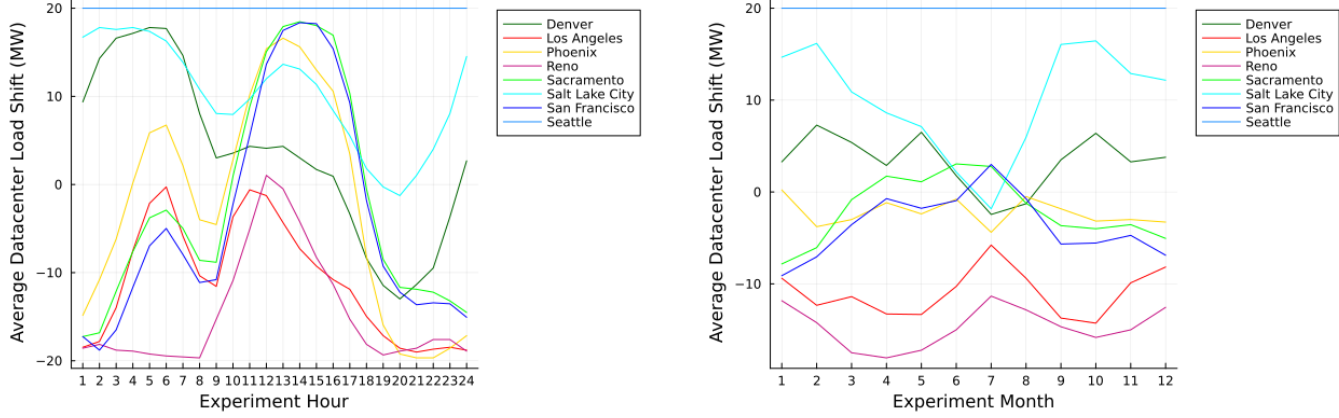


Figure 14: Average hourly (left) and monthly (right) load shift factors for each data center when rerunning experiment 1 with locational marginal pricing based shifting.

LMEs Provide Accurate Signals for Data Center and Generation Siting

Data Center Siting We consider the use of LMEs to understand the emissions impact of deciding siting static loads within a grid network. Here we randomly select a bus and a dispatch hour and observe how the overall system emissions change from adding a constant 200MW load, assumed to represent a large data center. The expected change in emissions at each experiment hour is given by the hourly LME multiplied by a 200MW load, while the realized change in system emissions is calculated by the difference between the overall system emissions with no additional load and the overall system emissions with the added 200MW load resulting from solving the DC optimal power flow dispatch. We perform this experiment for 1000 buses and dispatch periods chosen at random and observe the total realized change in emissions over the experimental horizon for all buses to be 1093.6 MT CO₂, or 114% of the expected change of 959.1 MT CO₂ from the total expected change in emissions, indicating that LMEs provide a fairly accurate estimate of system response for data center (and other similarly sized) load siting.

Generation Siting Finally, we consider the use of LMEs to understand the emissions impact of deciding siting generation within a grid network. Here we repeat the methodology from static load siting; however rather than adding a 200MW load we add a negative 200MW load to a bus to simulate a dispatched generation resource sized in the fashion of a large wind or solar generation resource. We again performed this experiment for 1000 buses and dispatch periods chosen at random and observed the total realized change in emissions to be -845.0 MT CO₂, totaling to 92.6% of the total expected change in emissions of 912.8 MT CO₂, again indicating LMEs provide an overall accurate estimate of system response for generation siting as well.

The siting experiments also serve to confirm consumer insights of the LME patterns, with consumption sources sited in the PNW and Montana causing significantly lower additional emissions than those sited elsewhere. Additionally, the siting of generation sources in the “Mountain West” regions leads to some of the highest magnitudes of emission displacement. Indeed, extrapolating these results to MT CO₂/MWh, a consumer building a 200 MW data center in the PNW would

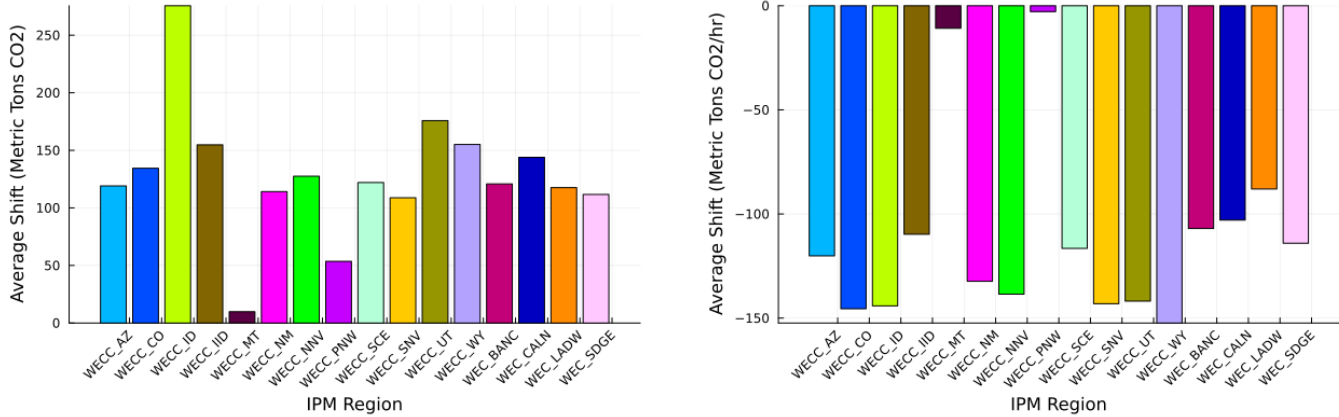


Figure 15: Average emissions shift from 200MW load (left) and generation (right) siting within each IPM region.

expect only to need to build a zero carbon resource that produces power at $\approx 67\text{MW}$ (assuming constant production over all hours) to have a net zero system level emission impact.

DISCUSSION

Insights for Data Center and Renewable Developers

The LME and accounting characteristics of the simulated WECC grid described in LMEs Reveal Three Regional Characteristics within WECC, LMEs Reflect Hourly and Seasonal Generation Characteristics, and LMEs Balance System Emissions and Reflect Entity Level Impacts provide significant insight into how data center operators can expect each of the three carbon intervention strategies to be most effective in reducing system emissions.

1. *The PNW and Montana regions have lowest LMEs for data center siting:* the stable, low LMEs of the PNW and Montana regions make such areas attractive options as operating sites for large energy consumers, such as data centers, looking to have a decreased carbon footprint. After these areas, the lower, sun-varied LMEs of “Sunbelt” regions, particularly those of northern California make these regions more attractive over the more consistent high-LME “Inter-Mountain West” regions.
2. *The Sunbelt regions are attractive for carbon-aware data center operation:* For data centers operating within the PNW and Montana regions, the stability of the low LMEs implies that there may be little to gain from consumption changes such as load shifting. However, for consumers operating outside these areas, particularly in the “Sunbelt” regions, the correlation between LME temporal patterns and solar strength indicates reliable opportunities to lower a data center’s carbon footprint via carbon-aware operation. In particular, operational changes, which shift loads toward high solar production and subsequent low LME hours and months in these regions, have a high potential to provide significant carbon benefits.
3. *The Inter-Mountain West regions have strong potential for carbon reduction projects:* For developers looking to take carbon reduction actions, the “Inter-Mountain West” regions exhibit strong potentials for such projects. The high LMEs of these regions combined with low intra-region transmission congestion and high potential for VRE resources leads to

likely strong system carbon reductions per unit of VRE capacity added within the regions. 371
Transmission upgrades between the PNW and Montana regions and the “Inter-Mountain 372
West” regions also exhibit strong potential for significant system carbon reductions through 373
the highly negative SCIs exhibited across such lines. 374

Insights for Policy Analysis

LME-based interventions show promise. There has been much policy discussion around 375
scope 2 accounting systems to improve upon existing issues and better align carbon-conscious 376
consumers such as the data center operators discussed above. Recent updates from the GHG 377
protocol working group have signaled interest in the use of LMEs as an improved evaluation 378
framework for consumer interventions²⁶. 379

Indeed, in Sections LMEs Provide Accurate Emission Signals for Data Center Operations and 380
LMEs Provide Accurate Signals for Data Center and Generation Siting, we observed that insight 381
from LMEs proved accurate at providing system response estimates for load siting, demand 382
response, and generation procurement actions, indicating that LME-based intervention strategies 383
and LME-based accounting can be powerful tools for aligning data center consumption with the 384
renewable transition. 385

Network representation and interconnection-scale simulation are important. It should be 386
noted that such accuracy findings contradict some previous studies¹⁴, where LME-based 387
demand response was found to have significantly lower accuracy than observed here. A key 388
difference between these studies was the size and scope of the network dispatch simulation. The 389
larger scale WECC simulation in our study seems to provide more stability to regional LMEs 390
with respect to significant load changes, comparing to simulations restricted to more local areas 391
such as California. This implies that, to properly align intervention actions with system response, 392
planners and operators must be careful to simulate their interventions on a power system with 393
sufficiently large scale and high spatial and temporal resolution. 394

Fine-grained simulation provides insights on tax credit policy. Furthermore, taking in 395
conjunction the observed accuracy of LMEs to describe system response and the observed LME 396
characteristics, we see the importance of fine-grained approaches to carbon accounting policies. 397
LMEs showed significant variance across often considered blanket policy regions such as FERC 398
Electricity Markets²⁷ (for example, Idaho and the PNW are both within the same Northwest 399
electricity market but experience drastically different LME characteristics), along with even individual 400
nodes exhibiting significant temporal variation. Such policy implications are broadly applicable 401
beyond just the WECC grid and can be used to evaluate the structure of current decarbonization 402
incentives. One particularly pertinent example is the green hydrogen tax credit, where hydrogen 403
producers operating in the “qualifying states” of Washington and California, having implemented 404
greenhouse gas cap programs, can qualify for green hydrogen tax credits without additional 405
energy procurement measures²⁸. Such a broad-scope state-level policy fits poorly with the 406
observed current LME trends where many nodes within California exhibit average LMEs close to 407
the level of natural gas carbon intensity, indicating that, despite the existence of emissions caps, 408
in the short term additional demand is met through increased fossil fuel consumption. Of course, 409
such an analysis does not account for the full complexities of such a policy - in this instance likely 410
including a desire to create political incentives for states to adopt emissions caps - however, it 411
does provide important insight into how such policies may be misaligned with the physical grid 412
response. 413

Recommendations for Regional Policy Makers.

415

Finally, to complete our exploration, we can consider the insights from Sections LMEs Reveal Three Regional Characteristics within WECC, LMEs Reflect Hourly and Seasonal Generation Characteristics, and LMEs Balance System Emissions and Reflect Entity Level Impacts through the lens of regional policymakers under the adoption of such LME-based accounting systems.

416

417

418

419

Regions with high penetration of firm low carbon power: For policymakers in these regions, the existing high frequency of low LMEs provides strong incentives for data centers to locate here and shift workloads to this area. Policy makers wishing to continue to provide such carbon incentives should ensure that the low carbon generation capacity remains sufficient to meet an increasing future load.

420

421

422

423

424

Regions with consistent marginal fossil fuels: Despite possibly containing a significant renewable capacity, the marginal responsibility of emissions from fossil fuel plants mean that data centers are disincentivized from locating workloads in these regions. Policy makers looking to attract data center operations should look to lower average LMEs through increasing the amount of time that carbon-free resources act as marginal generations through building out carbon-free generation capacity in the region. Such an increase could likely be achieved partially through carbon-free generation projects financed through data center development, as high regional LMEs likely make such areas attractive for energy procurement strategies.

425

426

427

428

429

430

431

432

Regions with high solar penetration: The variable LMEs present in these regions provide an opportunity for policy makers to use data center intervention actions to flatten the infamous duck curve present in high solar regions. In particular, the lower LMEs observed during peak solar production incentivize data centers performing LME-based workload shifting interventions to shift demand into hours of peak solar production, creating an overall more stable load profile when considering net demand with VRE resources removed. Such interventions may help improve grid resilience while simultaneously allowing for increased renewable deployment.

433

434

435

436

437

438

439

METHODS

440

Generation Dispatch

441

For each experiment, we run 8760 separate power dispatch problems, each simulating one hour of WECC system operation. To do so, we follow the LME calculation methodology similar to that of Rudkevich and Ruiz¹⁷ and use a combined dispatch and LME calculation model for the WECC grid. In particular, we form a feasible set of possible generation dispatches from the set of optimal solutions to the DC-OPF economic dispatch problem with load shedding:

442

443

444

445

446

$$DCOPF(P^D) := \min_{P^G, \theta, f} c_{gen}^T P^G + c_{shed} \cdot \|ls\|_1 \quad (\text{DCOPF Model})$$

$$\text{s.t. } B_{ij}(\theta_i - \theta_j) - f_\ell = 0, \quad \forall \ell = (i, j) \in L, \quad (7)$$

$$\sum_{g \in G_i} P_g^G - \sum_{\ell=(i,j) \in L} f_\ell + \sum_{\ell=(j,i) \in L} f_\ell - P_i^D + ls_i = 0, \quad \forall i \in N, \quad (8)$$

$$f_\ell \leq f_\ell^{max}, \quad \forall \ell \in L, \quad (9)$$

$$f_\ell \geq -f_\ell^{max}, \quad \forall \ell \in L, \quad (10)$$

$$P_g^G \leq P_g^{max}, \quad \forall g \in G, \quad (11)$$

$$P_g^G \geq P_g^{min}, \quad \forall g \in G, \quad (12)$$

$$ls_i \geq 0, \quad \forall i \in N, \quad (13)$$

$$ls_i \leq P_i^D, \quad \forall i \in N. \quad (14)$$

We then optimize over the feasible set of optimal solutions to the (DCOPF Model) by minimizing the secondary objective of system carbon emissions, allowing for the calculation of marginal emission characteristics for each dispatch hour. The resulting optimal power flow solution from this two-tier optimization defines the dispatch solution for each hour.

447

448

449

450

LME-Based Carbon Accounting Calculation

451

We apply the LME-based accounting scheme as described in Definition 2. Such accounts are calculated matching the results of Rudkevich and Ruiz¹⁷ using the LME and SCI values derived from the generation dispatch for each hour along with the load, generation, and flow values associated with the corresponding dispatch.

452

453

454

455

Additionally, for the most accurate picture of LME-based accounting within the WECC and to account for imperfections in our grid modeling methodology, we remove all high load shedding event hours from the accounting consideration, where high load shedding is considered to be an hour where load shedding is greater in magnitude than 100MWh.

456

457

458

459

Data Center Load Shifting

460

For the load shifting experiments described in LMEs Provide Accurate Emission Signals for Data Center Operations, we run three distinct optimization problems. First, the considered data center base loads are added to the corresponding WECC nodes across all 8760 dispatch periods and we rerun (DCOPF Model) in the manner of Generation Dispatch to define emissions and LME values in the “base case”. Second, we solve an emission minimizing load shifting problem across the data centers where each data center is allowed to increase or decrease its load by up to 20% in any given dispatch period subject to the constraint that the sum of the total load over all participating data centers throughout each day (a 24-hour window) must remain the same as in

461

462

463

464

465

466

467

468

the “base case”. This leads to 365 separate data center load dispatch problems whose objective describes the total expected emissions change for each day: 469
470

$$CO2SHIFT(LME) := \min_{\Delta} \sum_{t \in T, i \in DC} LME_{t,i} \Delta_{t,i} \quad (\text{Shifting Model})$$

$$\text{s.t.} \quad \sum_{t \in T, i \in DC} \Delta_{t,i} = 0 \quad (15)$$

$$\Delta_{t,i} \leq 0.2 \times DCSIZE \quad \forall t \in T, i \in DC \quad (16)$$

$$-\Delta_{t,i} \leq 0.2 \times DCSIZE \quad \forall t \in T, i \in DC \quad (17)$$

Finally, the resulting data center load shifts from the above problems are applied and the 8760 471
dispatch periods are reran with the shifted loads to define emissions in the “shifted case”. We 472
then subtract the total “shifted case” emissions from the “base case” emissions to generate the 473
realized emissions change. 474

RESOURCE AVAILABILITY

475

Lead contact

476

Requests for further information and resources should be directed to and will be fulfilled by the lead contact, Andy Sun (sunx@mit.edu).

477

478

Materials availability

479

This study did not generate new materials.

480

Data and code availability

481

Any information required to reanalyze the data reported in this paper is available from the lead contact upon request.

482

483

ACKNOWLEDGMENTS

484

The authors would like to thank the gift from Meta that in part supported this work and for the valuable reviews and comments from Hank He and Nikky Avila of the Global Energy Team at Meta. Additionally, L.C. was partially supported by the Dick and Jerry Smallwood Fellowship Fund during portions of this work. The authors would also like to thank Thomas Lee for the compilation and provision of WECC grid network and demand data.

485

486

487

488

489

AUTHOR CONTRIBUTIONS

490

Conceptualization, A.S. and L.C.; methodology, A.S. and L.C.; investigation, A.S. and L.C.; writing—original draft, L.C.; writing—review & editing, A.S. and L.C.; funding acquisition, A.S.; resources, A.S. and L.C.; supervision, A.S.

491

492

493

DECLARATION OF INTERESTS

494

The authors declare no competing interests.

495

DECLARATION OF GENERATIVE AI AND AI-ASSISTED TECHNOLOGIES

496

497

During the preparation of this work, the authors used Google Gemini in order to generate code scaffolding for plots and figures. After using this tool or service, the authors reviewed and edited the content as needed and take full responsibility for the content of the publication.

498

499

500

References

501

1. Cornish, C., Tauschinski, J., Webber, J., Stylianou, N., Xiao, E., Walker, O., and Bryan, K. (2025). Inside the AI race: can data centres ever truly be green? *Financial Times*. URL: <https://www.ft.com/content/0f6111a8-0249-4a28-aef4-1854fc8b46f1>. 502
503
504
2. EPA (2025). Ireland's Greenhouse Gas Emissions Projections 2023-2050. 505
3. Amazon (2025). Carbon-free energy - Amazon Sustainability. . URL: <https://sustainability.aboutamazon.com/climate-solutions/carbon-free-energy>. 506
507
4. Google (2016). Clean Energy: Buying Renewable Energy - Google Sustainability. . URL: <https://sustainability.google/stories/ppa/>. 508
509
5. Meta (2024). Data Centers. . URL: <https://sustainability.atmeta.com/data-centers/>. 510
6. Microsoft (2023). Measuring energy and water efficiency for Microsoft Datacenters. . URL: <https://datacenters.microsoft.com/sustainability/efficiency/>. 511
512
7. Cupelli, L., Schütz, T., Jahangiri, P., Fuchs, M., Monti, A., and Müller, D. (2018). Data Center Control Strategy for Participation in Demand Response Programs. *IEEE Transactions on Industrial Informatics* *14*, 5087–5099. URL: <https://ieeexplore.ieee.org/document/8293840/>. doi: 10.1109/TII.2018.2806889. 513
514
515
516
8. Giacobone, B. (2025). Google expands demand response to target machine learning workloads. . URL: <https://www.latitudemedia.com/news/google-expands-demand-response-to-target-machine-learning-workloads/>. 517
518
519
9. Gillenwater, M. (2008). Redefining RECs—Part 1: Untangling attributes and offsets. *Energy Policy* *36*, 2109–2119. URL: <https://www.sciencedirect.com/science/article/pii/S0301421508000803>. doi: 10.1016/j.enpol.2008.02.036. 520
521
522
10. Brander, M., Gillenwater, M., and Ascui, F. (2018). Creative accounting: A critical perspective on the market-based method for reporting purchased electricity (scope 2) emissions. *Energy Policy* *112*, 29–33. URL: <https://www.sciencedirect.com/science/article/pii/S0301421517306213>. doi: 10.1016/j.enpol.2017.09.051. 523
524
525
526
11. Bjørn, A., Lloyd, S.M., Brander, M., and Matthews, H.D. (2022). Renewable energy certificates threaten the integrity of corporate science-based targets. *Nature Climate Change* *12*, 539–546. URL: <https://www.nature.com/articles/s41558-022-01379-5>. doi: 10.1038/s41558-022-01379-5. Publisher: Nature Publishing Group. 527
528
529
530
12. Bjørn, A., Gebara, C.H., and Brander, M. (2025). Untangling deliverability, additionality and double counting related to renewable energy certificates for improved scope 2 emissions accounting. *Environmental Research Letters* *20*, 051006. 531
532
533
13. Xu, Q., Ricks, W., Manocha, A., Patankar, N., and Jenkins, J.D. (2024). System-level impacts of voluntary carbon-free electricity procurement strategies. *Joule* *8*, 374–400. URL: <https://linkinghub.elsevier.com/retrieve/pii/S2542435123004993>. doi: 10.1016/j.joule.2023.12.007. 534
535
536
537
14. Gorka, J., Rhodes, N., and Roald, L. (2025). ElectricityEmissions.jl: A Framework for the Comparison of Carbon Intensity Signals. *arXiv*. URL: <http://arxiv.org/abs/2411.06560>. doi: 10.48550/arXiv.2411.06560 arXiv:2411.06560 [eess]. 538
539
540

15. Knittel, C.R., Senga, J.R.L., and Wang, S. (2025). Flexible Data Centers and the Grid: Lower Costs, Higher Emissions?. National Bureau of Economic Research. URL: <https://www.nber.org/papers/w34065>. doi: 10.3386/w34065. 541

16. Sotos, M. (2015). Ghg protocol scope 2 guidance. World Resources Institute. Saatavilla 544
<https://ghgprotocol.org/scope-2-guidance>. 545

17. Rudkevich, A., and Ruiz, P.A. (2012). Locational Carbon Footprint of the Power Industry: 546
Implications for Operations, Planning and Policy Making. In Q.P. Zheng, S. Rebennack, 547
P.M. Pardalos, M.V.F. Pereira, and N.A. Iliadis, eds. Handbook of CO2 in Power Systems 548
pp. 131–165.. Berlin, Heidelberg: Springer. ISBN 978-3-642-27431-2 pp. 131–165. URL: 549
https://doi.org/10.1007/978-3-642-27431-2_8. doi: 10.1007/978-3-642-27431-2_8. 550

18. Avila, N., He, H., Rastegar, R., Tolan, J., Tiecke, T., and White, B. (2025). Catalyzing 551
System-level Decarbonization: An Analysis of Carbon Matching As An Accounting Frame- 552
work. arXiv. URL: <http://arxiv.org/abs/2511.19666>. doi: 10.48550/arXiv.2511.19666 553
arXiv:2511.19666 [math]. 554

19. Lee, T., and Sun, A. (2025). Canopi: Contingency-aware nodal optimal power investments 555
with high temporal resolution. arXiv preprint arXiv:2510.03484. 556

20. OpenStreetMap contributors (2017). Planet dump retrieved from <https://planet.osm.org> . 557
<https://www.openstreetmap.org> . 558

21. U.S. Energy Information Administration (2025). Form EIA-860 Annual Electric Generator 559
Report. Data set. . URL: <https://www.eia.gov/electricity/data/eia860/> accessed on 560
2025-07-08. Data for year 2024. 561

22. NOAA National Centers for Environmental Prediction, Environmental Modeling Cen- 562
ter (2016). Rapid refresh (rap) [20 km]. NOAA National Centers for Environmental 563
Information. URL: <https://www.ncei.noaa.gov/has/HAS.FileAppRouter?datasetname=RAPANL252&subqueryby=STATION&applname=&outdest=FILE> accessed on August 5, 2025. 564
565

23. Campbell, A. (2023). Form eia-930 data. . URL: <https://www.osti.gov/biblio/1963660>. 566
doi: 10.21947/1963660. 567

24. Benevento, A., and Durante, F. (2024). Correlation-based hierarchical clustering of time 568
series with spatial constraints. Spatial Statistics 59, 100797. URL: <https://linkinghub.elsevier.com/retrieve/pii/S2211675323000726>. doi: 10.1016/j.spasta.2023.100797. 569
570

25. Roberts, B. (2025). Data Center Infrastructure in the United States, 571
2025 (Map). URL: <https://research-hub.nrel.gov/en/publications/data-center-infrastructure-in-the-united-states-2025-map>. 572
573

26. Huckins, S. (2025). Scope 2 Standard Advances: ISB Approves Consultation 574
on Market- and Location-Based Revisions; Signals Cross-Sectoral Work Ahead 575
on Avoided Emissions | GHG Protocol. . URL: <https://ghgprotocol.org/blog/scope-2-standard-advances-isb-approves-consultation-market-and-location-based-revisions>. 576
577

27. FERC (2025). Electric Power Markets. . URL: <https://www.ferc.gov/electric-power-markets>. 578
579

28. Service, I.R. (2025). Credit for Production of Clean Hydrogen and Energy 580
Credit. . URL: <https://www.federalregister.gov/documents/2025/01/10/2024-31513/credit-for-production-of-clean-hydrogen-and-energy-credit>. 581
582